JOURNAL OF AIRCRAFT
Vol. 46, No. 2, March–April 2009

Engineering Notes

ENGINEERING NOTES are short manuscripts describing new developments or important results of a preliminary nature. These Notes should not exceed 2500 words (where a figure or table counts as 200 words). Following informal review by the Editors, they may be published within a few months of the date of receipt. Style requirements are the same as for regular contributions (see inside back cover).

Design of a High-Lift System with Droop Nose Device

Adam Jirásek* and Olivier Amoignon†
FOI, Swedish Defence Research Agency, SE-164 90 Stockholm, Sweden

DOI: 10.2514/1.41520

I. Introduction

THE realization of wings with an extended portion of laminar flow, such as is being designed in the European project New Aircraft Concept Research (NACRE), imposes to use high-lift systems that preserve the smoothness of the wing as far downstream as possible. Our choice was to develop a system equipped with a single slotted trailing-edge flap and a morphing droop nose device. A similar concept was earlier presented by Morgan [1], and high-lift systems with a droop nose bending around a hinge line were also studied by Khodadoust and Washburn [2] and Khodadoust and Shmilovich [3]. In the next section we use a design of experiment (DOE) approach, starting from a general description of the high-lift airfoil consisting of 12 parameters. Five of them were selected and optimized by a response surface method. The performance of the best candidate is analyzed in a third section and compared there with a high-lift system equipped with a vented Krueger leading-edge flap. In the fourth section a flow control system with vortex generators (VG) is investigated in order to improve the overall performance of the high-lift system with flexible droop nose device.

II. Baseline and Optimization by Design of Experiment Approach

The shape of the deployed droop nose (Fig. 1) is defined by its maximum length (l_{DN}), its angle of deflection (α_{DN}), and its leading-edge extension (Δx_{DN}). Supposing that the front spar is located at 20% of the chord, we use this value for l_{DN}. A spoiler at the trailing edge of the main airfoil can also be slightly deflected, which is defined by the parameter Δy_{SP}. The flap has a circular leading edge and the remaining parts are described by a spline (two parameters p_1 and p_2) and portions of the clean airfoil being further defined by l_{FU} and l_{FL} (Fig. 1). The position of the flap is given by the flap overhang Δx_{FO}, the gap between the main airfoil and the flap (D_{gap}), and the flap deflection angle (α_{FL}), see Fig. 2.

Received 9 October 2008; revision received 16 December 2008; accepted for publication 16 December 2008.

*Currently at United States Air Force Academy, Colorado Springs, CO 80840. Member AIAA.
†Researcher, Department of Systems Technology.

A. Design with Design of Experiment Approach

The meshes are automatically generated for each set of design parameters using a commercial software package (IcemCFD) to create an Euler mesh that is used as input to an in-house code TRITET [4] that generates a suitable mesh for Reynolds-averaged Navier–Stokes (RANS) computations. The RANS equations are solved in Edge, FOI's in-house computational fluid dynamics (CFD) program package [5], using the Hellsten k–ω explicit algebraic Reynolds-stress turbulence model [6]. The flow around the high-lift airfoil is solved in $2.5D$, meaning that it models the flow around an infinite swept wing with sweep angle $\phi = 17.2$ deg. Convergence is accelerated by pseudotime stepping and full multigrid (see Fig. 3).

A DOE approach [7,8] is used to find the best parameters for the high-lift system.

B. Screening

The screening matrix was the R^{IV} resolution matrix and the intervals of the parameters are given in Table 1. The Pareto graphs in Fig. 4 indicate the sensitivities of lift and drag coefficients with respect to the parameters of design. The parameters that have the largest effect on the lift are the flap overhang Δx_{FO}, the length of the lower side l_{FL}, the flap shape parameters (p_1, p_2), and the size of the gap between the main airfoil and the flap D_{gap}. The flap deflection α_{FL} had a relatively small effect but it influences other design parameters. The two most significant parameters for the drag are the droop nose angle α_{DN} and the flap deflection angle α_{FL}. To summarize, the selected parameters are the flap overhang Δx_{FO}, the length of the lower side l_{FL}, the size of the gap between the main airfoil and the flap D_{gap}, the flap deflection α_{FL}, and the droop nose angle α_{DN}.

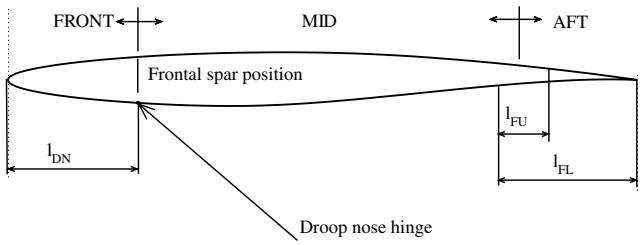

Fig. 1 Baseline airfoil with parameters for high-lift device definition.

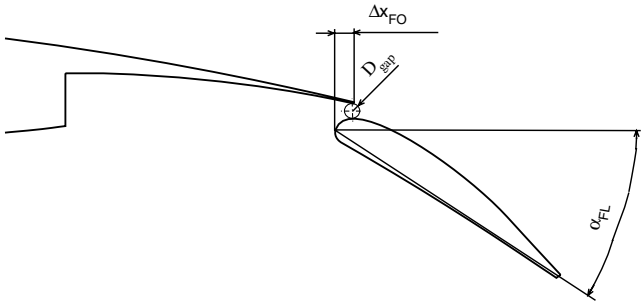

Fig. 2 Parameterization of the flap settings.

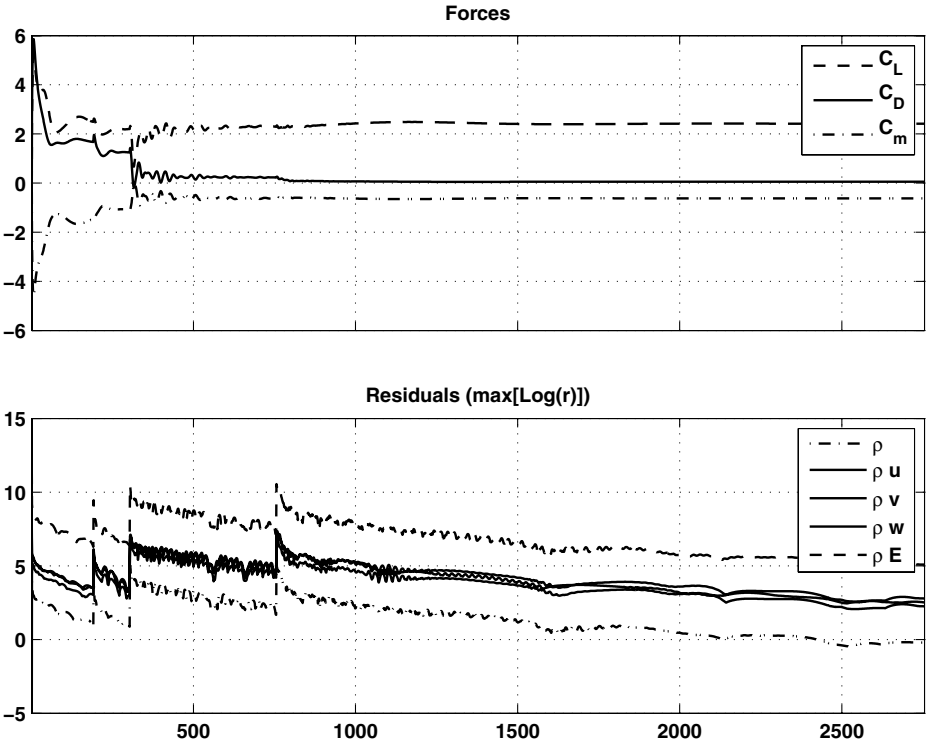

Fig. 3 Convergence for the HLS1 configuration at angle of attack 12 deg.

C. Modeling

The response surface is a second-order model containing primary effects, their interaction, and quadratic effects for arbitrary k input factors x_i and output variable y

$$y = \beta_0 + \sum_{j=1}^{k} \beta_j x_j + \sum_{j=1}^{k} \beta_j x_j^2 + \sum_{j=2}^{k} \sum_{j=1}^{i<j} \beta_{ij} x_i x_j \qquad (1)$$

The input factors x_j are the five parameters selected above, and the output variable y represents lift coefficient c_L. The coefficients β_j and β_{ij} in Eq. (1) along with an interval of confidence were obtained by least squares and t test on individual regression coefficients with the level of confidence 95%. The optimal geometry was located at a corner of the design space, indicating that improvements are possible at the cost of violating the upper bound constraints on the length of the spoiler and the angle of the flap.

III. Performances

The selected airfoil is referred to as the high-lift system (HLS1) configuration (see Fig. 5). Its 25%c long flap is deflected at $\alpha_D = 42$ deg. In Fig. 6 the 2.5D lift curve of HLS1 drops at an angle of attack $\alpha = 16$ deg and above due to flow separation on the spoiler.

Table 1 High-lift profile design variables

Design parameter	Upper limit	Lower limit
Droop nose deflection angle α_{DN}, deg	0	30
Droop nose extension Δx_{DN}, %c	0	10
Deflection of spoiler Δy_{SP}, %c	0	1.5
Flap overhang Δx_{FO}, %c	−1	1
Flap-shroud gap D_{gap}, %c	1	2.5
Flap deflection angle α_{FL}, deg	20	40
Flap lower side length l_{FL}, %c	15	25
Flap upper side length l_{FU}, %c	10	12
Flap leading edge radius R_{LE}, %c	1.2	1.5
Flap circular leading edge radius angle α_{LE}, deg	50	80
Parameter of spline p_1	0.01	0.03
Parameter of spline p_2	0.08	0.12

In the same figure the polar for HLS1 has a kink in front of the maximum lift point. This is due to the flow being separated on the flap at angles of attack below 11 deg, whereas it is attached at larger angles.

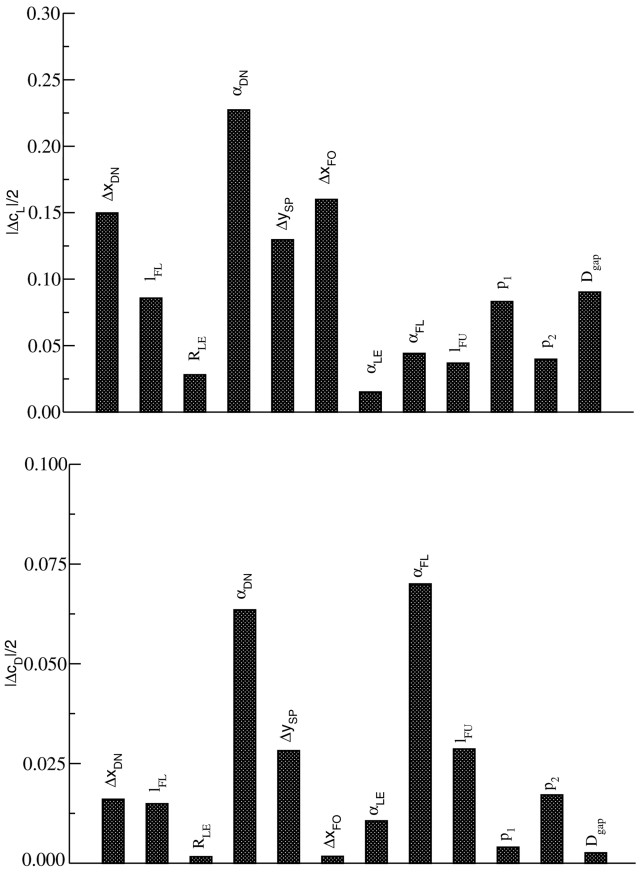

Fig. 4 Pareto graphs with main effects.

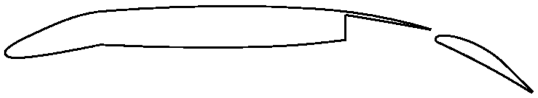

Fig. 5 HLS1 configuration.

A. Effect of Droop Nose Size

The system HLS1 was designed assuming a 20% long droop nose, corresponding to the position of the front spar. The comparison with a 15% long droop nose, deflected with the same angle, slightly reduces the maximum lift $\Delta c_L = 1.2\%$. The main effects are the increase of the lift at low angles of attack and a decrease at high angles of attack (see Fig. 7).

B. Comparison with a Krueger Flap

The integration of the proposed system may be challenging, for example, near the wing–fuselage junction where the induced angle of attack requires that the high-lift system accepts large angles of attack without massive flow separation. A solution that can preserve the smoothness of the shape on the suction side is the Krueger flap. The

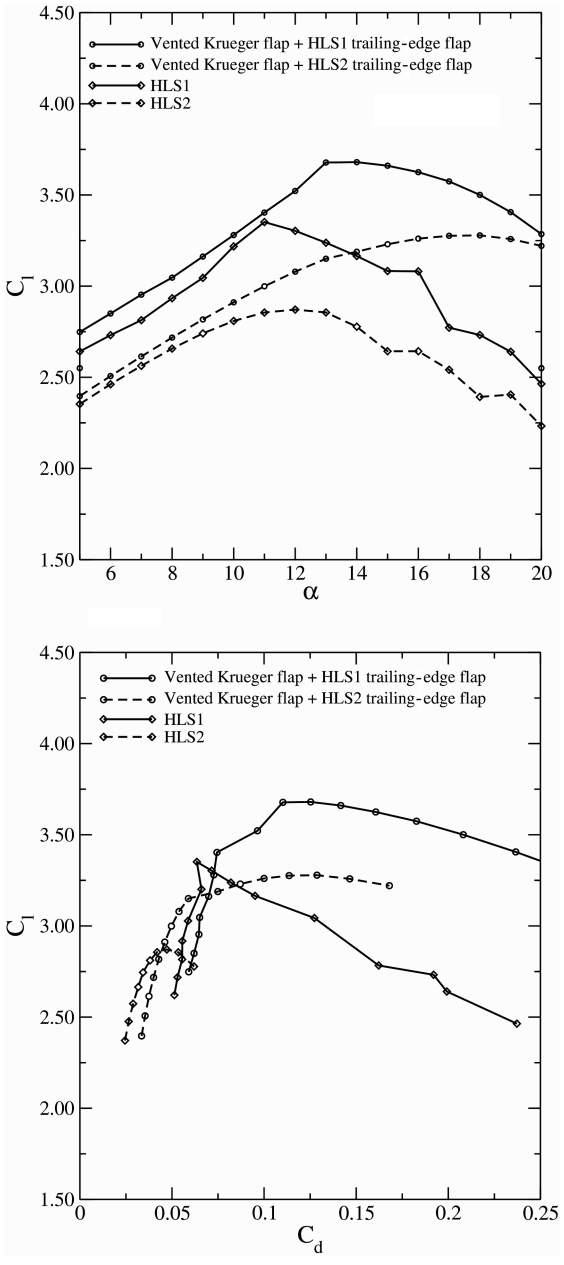

Fig. 6 Lift and polar curves.

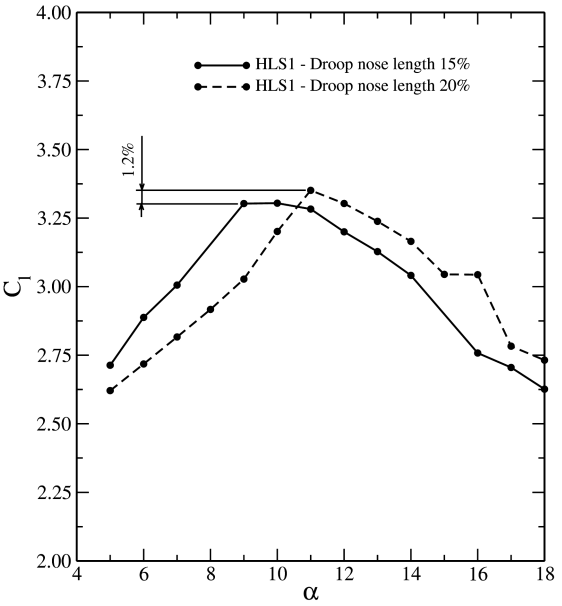

Fig. 7 Lift curves of the HLS1 geometry with modified length of droop nose l_{DN}.

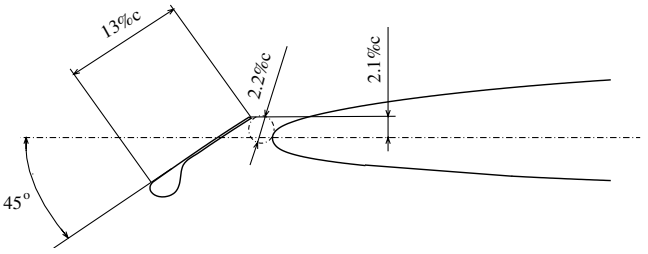

Fig. 8 Airfoil with Krueger flap.

Krueger flap investigated here is 15%c long (Fig. 8) and the cavity accommodating the Krueger flap is located downstream of the possible stagnation points at cruise. The position and deflection angle of the vented Krueger flap are shown in Fig. 8 and were set similarly to the one designed here [9]. Figure 6 shows the lift curve and polar of the airfoil with droop nose and Krueger flap along with polars of our best droop nose (HLS1) high-lift system. At angles of attack lower than 11 deg, the presence of the Krueger flap improves the lift relative to HLS1. The improvement in lift is probably due to the greater visible surface when the Krueger flap is deployed. This improvement involves though a larger drag. However, the lift obtained with the vented Krueger for angles larger than 11 deg is larger than the maximum lift obtained with the HLS1 configuration for angles up to 20 deg, see Fig. 6, which is the main benefit from this hybrid solution.

IV. Flow Control with Vortex Generators

The performance of the high-lift HLS1 can also be improved controlling the flow on the flap. For this purpose the flap can be equipped with corotating triangular VGs as in [10]. The flow control devices are located on the suction side of the flap at 40% of the chord, and their height is 25% of the boundary-layer thickness and the vanes make a 16 deg angle with the freestream. For the determination of

Table 2 Updated values of lift and drag with flow control

Angle of attack	Δc_L[%]	Δc_D[%]	VG configuration
10°	+5.9	−23.9	Flap
15°	+2.9	−15.6	Flap + Spoiler
18°	+1.9	−7.5	Flap + Spoiler

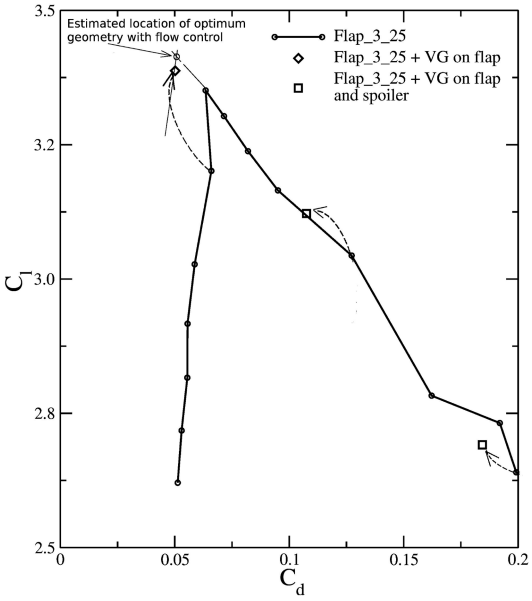

Fig. 9 Polar of the high-lift system without and with flow control.

their position and size we refer to [11]. The CFD with vortex generators is performed using the *jBAY* model, which is described in [10,12]. The location of the VGs under the spoiler, when the flap is retracted, prevents disturbing the flow around the clean airfoil.

The VGs used here prevent flow separation, thus reducing the drag and increasing the lift at the angles of attack listed in Table 2 (see also Fig. 9). Table 2 shows the relative changes of lift and drag for the HLS1 configuration at three angles of attack with flow control compared to the high-lift system without flow control.

V. Conclusions

A high-lift system with a droop nose device, a Fowler flap, and a hinged spoiler was designed using 2.5*D* CFD (RANS) analysis and a design of experiment approach. The main aim was to investigate one of the candidate systems that could enhance the performance of laminar wings at landing and takeoff. Some aspects of the integration were also discussed, such as the influence of the droop nose size and the use of a Krueger flap in place of the droop nose. A shorter droop nose increases the lift by up to 9% at angles of attack below 11 deg for a loss of maximum lift of only 1.2%, whereas the substitution of the droop nose device by a conventional vented Krueger flap would increase the lift at high angles of attack. Finally, flow control with vortex generators is investigated as a means to improve the flow on the flap which otherwise tends to be separated at angles of attack close to the angle of maximum lift.

Acknowledgment

This work was financed by the European Commission under the European project New Aircraft Concept Research, NACRE. The authors would like to acknowledge Lasse Tyssel, Ulf Tengzelius, Ola Hamnér, and Per-Åke Torlund from FOI.

References

[1] Morgan, H. L., "High-Lift Flaps for Natural Laminar Flows Airfoils," *Laminar Flow Aircraft Certification*, NASA CP-2413, May 1986.

[2] Khodadoust, A., and Washburn, A., "Active Control of Flow Separation on a High-Lift System with Slotted Flap at High Reynolds Number," AIAA Paper 2007-4424, June 2007.

[3] Khodadoust, A., and Shmilovich, A., "High Reynolds Number Simulations of Distributed Active Flow Control for a High-Lift System," AIAA Paper 2007-4423, June 2007.

[4] Tyssel, L., "Hybrid Grid Generation for Complex 3D Geometries," *Proceedings of the 7th International Conference on Numerical Grid Generation in Computational Field Simulation*, Whistler, British Columbia, Canada, Sept. 2000, pp. 337–346.

[5] Eliasson, P., "EDGE, a Navier-Stokes Solver for Unstructured Grids," *Proceedings to Finite Volumes for Complex Applications III*, ISBN 1 9039 9634 1, ISTE Ltd., London, 2002, pp. 527–534.

[6] Hellsten, A., "New Advanced k-ω Turbulence Model for High Lift Aerodynamics," *AIAA Journal*, Vol. 43, No. 9, Sept. 2005, pp. 1857–1869.
doi:10.2514/1.13754

[7] Myers, R. H., and Montgomery, D. C., *Response Surface Methodology*, 3rd ed., Wiley, New York, 1995.

[8] Schmidt, R., and Laundsby, T., *Understanding Design of Experiment*, Air Academy Associates, Colorado Springs, CO, 1995.

[9] "High Reynolds Number Hybrid Laminar Flow Control (HLFC) Flight Experiment II. Aerodynamic Design," Boeing Commercial Airplane Group, Seattle, WA, NASA/CR-1999-209324, Sept. 1999.

[10] Lynn, R., and Tengzelius, U., "C5.2 Short-Chord Flaps," HELIX/TR/QinetiQ/C5.2/RL150803/2, EU Project Helix Report, 2003.

[11] Jirásek, A., "Design of Vortex Generator Flow Control in Inlets," *Journal of Aircraft*, Vol. 43, No. 6, Nov.–Dec. 2006, pp. 1886–1892.
doi:10.2514/1.21364

[12] Jirásek, A., "Vortex-Generator Model and Its Application to Flow Control," *Journal of Aircraft*, Vol. 42, No. 6, Nov.–Dec. 2005, pp. 1486–1491.
doi:10.2514/1.12220